Data in brief 29 (2020) 105243

Contents lists available at ScienceDirect

Data in brief

journal homepage: www.elsevier.com/locate/dib

Data Article

Data on molecular docking of naturally occurring flavonoids with biologically important targets

Anguraj Moulishankar*, Karthikeyan Lakshmanan

Department of Pharmaceutical Chemistry, KMCH College of Pharmacy, Coimbatore-48, Tamil Nadu, India

ARTICLE INFO

Article history:
Received 20 September 2019
Received in revised form 15 January 2020
Accepted 28 January 2020
Available online 4 February 2020

Keywords:
Molecular docking
Flavonoids
Antimicrobial
Anti-cancer
Anti-inflammatory
Glide
Schrodinger maestro

ABSTRACT

Flavonoids in nature are known to possess various activities such as anti-inflammatory, antimicrobial, anticancer, antioxidant, neuroprotective, anti-HIV activities etc., The molecular docking was performed by 26 naturally occurring flavonoids with selected targets COX-2, hydroxyacyl-ACP dehydratase, tyrosinase from *Agaricus bisporus*, isomaltase from *Saccharomyces cerevisiae*, Human IkB kinase beta, Human ABC transporter, topoisomerase II, topoisomerase IV, N-myristoyltransferase from *Candida albicans*, Peptide deformylase from *Pseudomonas aeruginosa*, polypeptide deformylase from *Streptococcus pneumoniae*. The analysis was based on docking score, glide energy, interactions type (bond type and distance) and interaction with amino acids. The top 5 flavonoids with best docking score was reported. The *in-silico* results provided for 26 naturally occurring flavonoid shows that they reduce the risk of inflammation, cancer and infectious disease if people have taken in diet continuously. The provided docking data of flavonoids may be useful to synthesis novel drug candidate for the mentioned targets.

* Corresponding author.
E-mail address: msanguraj1997@gmail.com (A. Moulishankar).

https://doi.org/10.1016/j.dib.2020.105243

Specifications Table

Subject	Pharmaceutical Science
Specific subject area	Interdisciplinary field includes organic chemistry, biochemistry, and biology. Drug design and discovery from plant sources.
Type of data	Tables Figures
How data were acquired	Schrodinger Maestro release 2018-4
Data format	Raw and Analysed
Parameters for data collection	The docking score, glide energy and interactions of protein with the ligand.
Description of data collection	The Proteins were collected from rcsb wwPDB. The flavonoids structures were obtained from Pubchem online database. The docking was done using glide software.
Data source location	https://www.rcsb.org/ https://pubchem.ncbi.nlm.nih.gov/
Data accessibility	PDB files of the chosen enzyme targets are publically available at https://www.rcsb.org/ Tables and Figures of the docking are accessible in the article.

Value of the Data

- The screening procedure enable the researchers to rapidly identify active natural compounds which can modulate a particular biochemical pathway.
- The screening results help to study the interaction/role of a bioactive flavonoid in a particular biochemical process at cellular level and provide preliminary ideas for drug design development
- By using this *in-silico* docking data, novel synthetic analogues with improved bioactivity and minimized side effects can be developed against these targets and research time can be minimized considerably.
- We select these 26 flavonoids because these are abundant in nature and well explored. Among these 26 flavonoids, the compounds which shows best affinity for various targets are shortlisted.
- The data also useful for research scholars who does not have the sufficient software and hardware requirements which not affordable by them.
- Research scholars, researchers in pharmaceutical chemistry can be benefit from the data.

1. Introduction

Flavonoids are a group of bioactive compounds which are extensively found in foodstuffs of plant origin. These are plant pigments synthesized from phenylalanine and generally display marvelous colors to the flowering parts of plants. Flavonoids comprise a large group of poly phenolic compounds, characterized by a benzo-4-pyrone structure, which is ubiquitous in vegetables and fruits. More than 9000 flavonoids have been reported in the literature and are present in different types and parts of plants such as vegetables, fruits, grains, legumes, beans, herbs, roots, leaves, seeds etc. The core structure of flavonoids has a three-ring diphenyl-propane (C6−C3−C6) unit, a fifteen-carbon skeleton. The flavonoid contains two benzene rings (A ring and B ring) which are connected by a C3 moiety. The C3 moiety forms a six-membered heterocyclic ring (ring C) attached to ring A. Regular consumption of flavonoids reduces the risk of a number of chronic diseases, including cancer, cardiovascular disease, diabetes, arthrosclerosis, neurodegenerative disorders, anti-ageing, anti-inflammatory, antiallergic, antiviral, and free radical scavenging. Among dietary sources of flavonoids, there are fruits, vegetables, nuts, seeds and spices. So, the provided docking data of flavonoid may be useful to synthesis novel drug candidate for the mentioned targets.

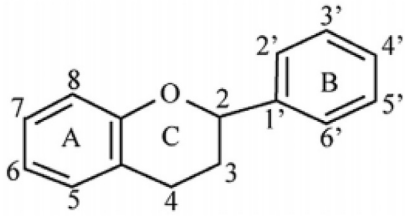

Table 1
List of Targets. Shows the PDB ID, resolution and description of the proteins selected for docking with the naturally occurring flavonoids.

S.No	PDB ID	Resolution (Å)	Description
1	3LN0	2.20	Structure of compound 5c-S bound at the active site of COX-2 [1]
2	4KIK	2.83	Human IkB kinase beta [2]
3	2XCS	2.10	The crystal structure of *Staphylococcus aureus* Gyrase complex with GSK299423 and DNA [3]
4	4HZ5	2.70	Pyrrolopyrimidine inhibitors of DNA gyrase b and topoisomerase iv, part i: structure guided discovery and optimization of dual targeting agents with potent, broad-spectrum enzymatic activity [4]
5	4RLJ	1.75	Crystal Structure of (3R)-hydroxyacyl-ACP dehydratase HadAB hetero-dimer from *Mycobacterium tuberculosis* [5]
6	1IYL	3.20	Crystal Structure of *Candida albicans* N-myristoyltransferase with Non-peptidic Inhibitor [6]
7	1LRY	2.60	Crystal Structure of *Pseudomonas aeruginosa* Peptide Deformylase Complexed with Antibiotic Actinonin [7]
8	2AIE	1.70	*Streptococcus pneumoniae* polypeptide deformylase complexed with inhibitor [7]
9	2Y9X	2.78	Crystal structure of PPO3, a tyrosinase from *Agaricus bisporus*, in deoxy-form that contains additional unknown lectin-like subunit, with inhibitor tropolone [8]
10	3A4A	1.60	Crystal structure of isomaltase from *Saccharomyces cerevisiae* [9]
11	6FFC	3.56	Structure of an inhibitor-bound human ABC transporter [10]

2. Data

In this article Table 1 provides the details about the targets and their description. Table 2 provide the structure of the naturally occurring flavonoids and plant sources. Table 3 gives docking score, glide

Table 2
List of Flavonoids. This table exemplifies the plant sources of the naturally occurring flavonoids, so that the compounds may be isolated and used for the research purposes.

S.No	Name of the flavonoid	Major plant source	Structure
1	Dabinol	*Dalbergia latifolia*	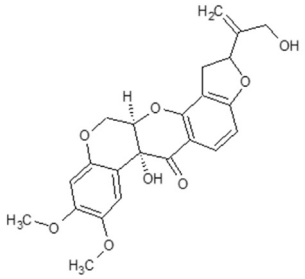
2	5HMF	*Citrus X sinensis*	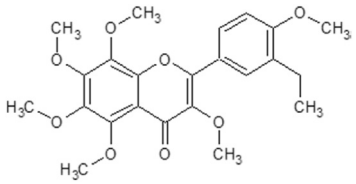

(*continued on next page*)

Table 2 (*continued*)

S.No	Name of the flavonoid	Major plant source	Structure
3	6a,12a-Dehydroamorphigenin	*Dalbergia sissoo*	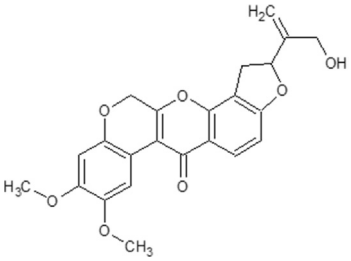
4	Afromosin	*Centrosema pubescens*	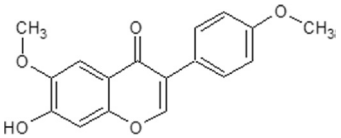
5	Amorphigenin	*Dalbergia cochinchinensis*	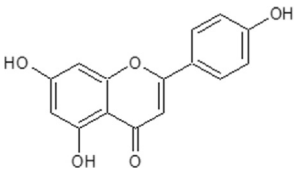
6	Biochanin- A	*fusarium javanicum*	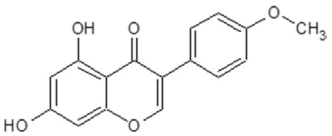
7	Catechin	*Camelia sinensis*	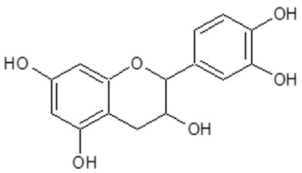
8	Chrysin	*Scutellaria baicalensis*	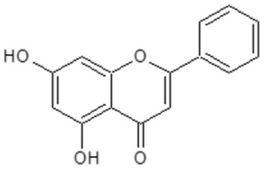

energy, interaction type and bond length of the docking. The 3D and 2D interactions of the high scored flavonoids with the target enzymes are shown in Figs. (1-7).

Table 2 (*continued*)

S.No	Name of the flavonoid	Major plant source	Structure
9	Demethylnobiletin	*Citrus depressa*	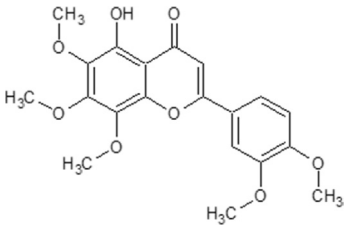
10	Epicatechingallate (ECG)	*Vicia faba*	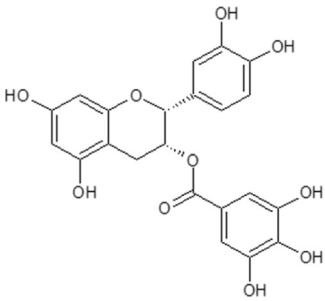
11	Epigallocatechin	*Camellia sinensis*	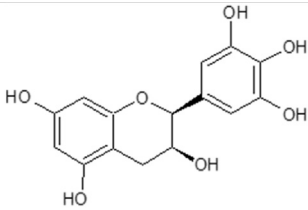
12	Epigallocatechingallate (EGCG)	*Camellia sinensis*	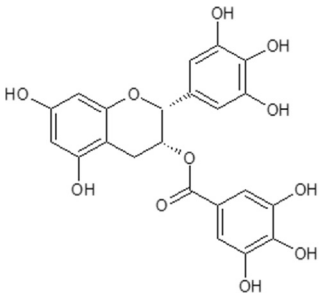
13	Floretin (Phloretin)	*Manchurian apricot.*	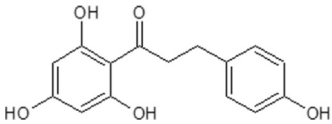

(*continued on next page*)

Table 2 (*continued*)

S.No	Name of the flavonoid	Major plant source	Structure
14	Formononetin	*Trifolium pratense*	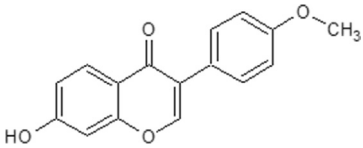
15	Hesperidin	*Citrus aurantium*	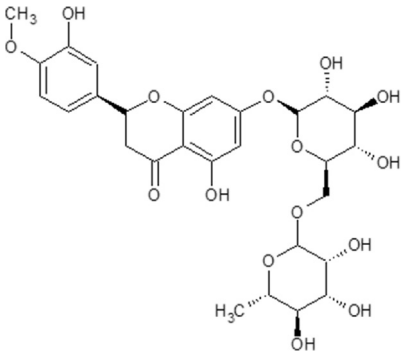
16	Morin	*Antiaris toxicaria*	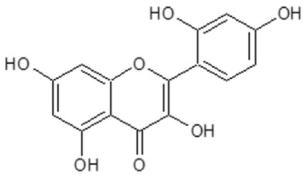
17	Naringenin	*Citrus paradisi*	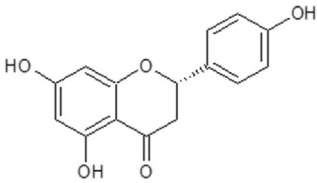
18	Naringin	*Citrus paradisi*	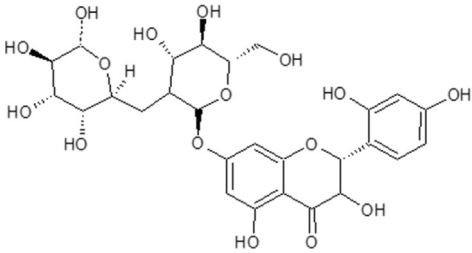

Table 2 (*continued*)

S.No	Name of the flavonoid	Major plant source	Structure
19	Neohesperidin	*citrus aurantium*	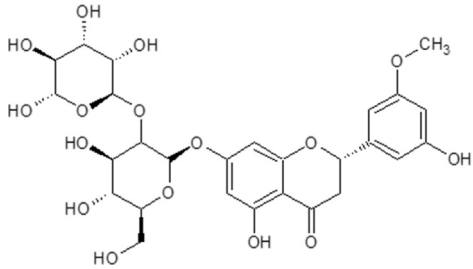
20	Quercetin	*Malus domestica*	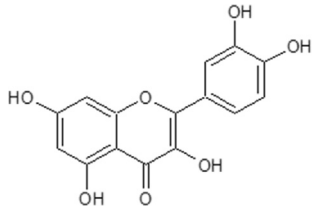
21	Robinin	*Vinca erecta*	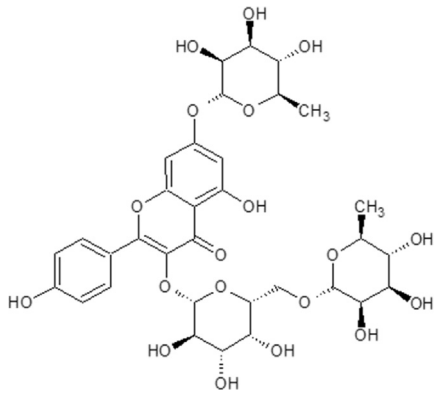
22	Rotenone	*Pachyrhizus erosus*	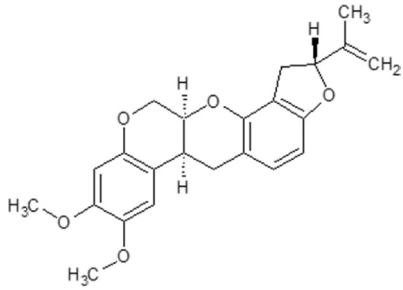

(*continued on next page*)

Table 2 (*continued*)

S.No	Name of the flavonoid	Major plant source	Structure
23	Sakuranetin	*Polymnia fruticosa*	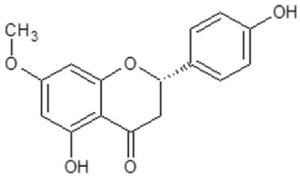
24	Silymarin	*Silybum marianum*	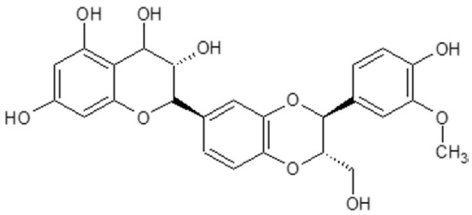
25	Nobiletin	*Citrus Unshiu*	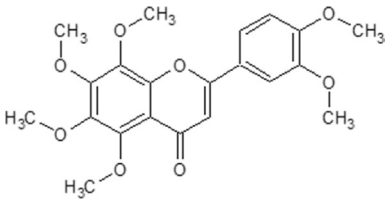
26	Kaempferol	*Allium cepa*	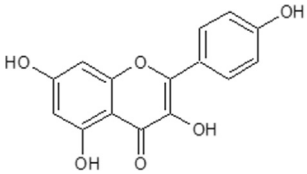

3. Experimental design, materials, and methods

3.1. Protein selection and preparation

The crystal structures of the selected proteins were retrieved from protein data bank. (PDB database, www.rcsb.org). The downloaded protein structure was prepared prior to docking using Schrodinger Maestro release 2018-4. Protein preparation was done by preprocessing the structures by assignment of bonds and bond orders, addition of hydrogens, filling in missing loops or side chains, capping uncapped C and N termini, adjusting bonds and formal charges for metals, and correcting mislabeled elements, removing water molecules, removing unwanted chains and optimization of hydrogen bonded structures followed by minimization.

3.2. Ligand preparation and molecular docking

The structures of the selected 26 flavonoids were downloaded from Pubchem https://pubchem.ncbi.nlm.nih.gov/) and saved in mol format. The energy minimization was done using Ligprep. The

Table 3
Docking score, Glide energy and Protein-Ligand Interactions. The docking score, Glide energy, interacting residues, type of interactions, bond length between residues and ligands are shown for each protein mentioned in Table 1.

Title	Docking Score	Glide Energy (Kcal/mol)	Interactions	Type	Bond length (Å)
Protein ID: 2XCS Antibacterial by gyrase inhibition					
Robinin	−8.03	−84.11	Asp A:1083	H-bond	2.03
			Asp A:1080	Ar-H-bond	2.20
			Glu A:1088	2 H-bond	1.73, 1.93
			Arg A:1122	2 H-bond	2.17, 2.61
Naringin	−7.85	−62.60	Lys 581	H-bond	2.43
			Asp 1083	Ar-H-bond	2.63
Neohesperidin	−7.72	−70.99	Asp 1083	H-bond	1.90
Silymorin	−7.29	−44.08	Glu 1088	H-bond	2.04
			Ala 1120	H-bond	2.17
			Tyr 1087	Ar-H-bond	2.70
Hesperidin	−7.25	−68.40	Arg 1122	H-bond	2.29
Protein ID: 4KIK Anticancer by IkB kinase inhibition					
Sakuranetin	−9.73	−44.98	Asp A:166	H-bond	1.45
			Glu A:97	H-bond	2.40
			Cys A:99	H-bond	2.04
Naringenin	−9.53	−43.50	Glu A:97	H-bond	2.42
			Cys A:99	H-bond	2.04
			Asp A:166	H-bond	1.45
Kaempferol	−9.33	−45.40	Lys A:44	H-bond	2.04
			Asp A:166	H-bond	2.16
			Cys A:99	H-bond	2.02
Naringin	−9.07	−59.59	Asp A:145	H-bond	1.78
			Lys A:147	H-bond	2.22
			Asp A:166	H-bond	1.87
			Glu A:97	H-bond	1.87
			Glu A:97	Ar-H-bond	2.48
			Cys A:99	H-bond	2.07
Morin	−9.03	−46.84	Asp A:166	H-bond	2.09
			Lys A:44	H-bond	2.02
			Cys A:99	H-bond	2.01
Protein ID: 4HZ5 Antibacterial by DNA gyrase b and topoisomerase IV inhibition					
Phloretin	−7.06	−50.83	Asp 26	H-bond	1.87
			HOH 407	H-bond	2.77
			HOH 408	H-bond	1.77
			HOH 401	H-bond	2.95
Catechin	−6.93	−45.78	Gly 80	H-bond	2.38
			Asp 76	H-bond	1.78
			HOH 427	H-bond	1.64
Morin	−6.92	−51.77	Asp 76	H-bond	1.59
			Asp 76	Ar-H-bond	2.36
			Gly 80	H-bond	2.45
Kaempferol	−6.75	−47.93	Gly 80	Ar-H-bond	2.40
			Asp 76	H-bond	1.60
Sakuranetin	−6.49	−41.60	Asp 76	H-bond	1.81
			Gly 80	H-bond	2.69
			HOH 401	H-bond	2.12
Protein ID: 2Y9X Antifungal (*Agaricus bisporus*) by tyrosinase inhibition					
Epigallocatechingallate	−7.22	−51.13	Arg 268	Pi-cation	6.02
			Asn 260	Ar-H-Bond	2.66
			Phe 264	Ar-H-Bond	3.12
Chrysin	−7.20	−34.87	His 259	Ar-H-Bond	3.63
			Hid 85	Ar-H-Bond	3.25
Kaempferol	−7.02	−35.15	Hie 244	Ar-H-Bond	3.02
			Arg 268	Pi-cation	5.66
Quercetin	−6.75	−34.47	Asn 260	Ar-H-Bond	2.77
			Arg 268	Pi-cation	2.89
Catechin	−6.67	−32.30	Arg 268	Pi-cation	6.19
Protein ID: 3LN0 Anti-inflammatory by cyclo-oxygenase inhibition					
Sakuranetin	−7.31	−31.36	Ser 516	H-Bond	2.67

(*continued on next page*)

Table 3 (*continued*)

Title	Docking Score	Glide Energy (Kcal/mol)	Interactions	Type	Bond length (Å)
Quercetin	−7.00	−34.33	Try 371	Ar-H-Bond	3.08
			Try 371	H-Bond	2.72
			Gly 178	H-Bond	2.71
Naringenin	−6.99	−30.27	Ser 516	H-Bond	2.62
Morin	−6.98	−35.14	Try 371	H-Bond	2.38
			His 75	Ar-H-Bond	3.00
			Tyr 341	Ar-H-Bond	2.51
			Arg 106	Pi-cation	7.60
Kaempferol	−6.91	−33.28	Tyr 371	Ar-H-Bond	3.50
			Tyr 371	H-Bond	2.24
Protein ID: 4RLJ Antituberculosis (*Mycobacterium tuberculosis*) by hydroxyacyl-ACP dehydratase inhibition					
Catechin	−7.47	−39.00	HOH 322	H-Bond	1.84
			HOH 312	H-Bond	2.14
Biochanin A	−6.95	−32.44	Gln 86	Ar-H-Bond	2.63
			HOH 322	H-Bond	1.73
Quercetin	−6.76	−39.63	HOH 322	H-Bond	1.88
Chrysin	−6.60	−32.57	Gln 86	H-Bond	2.65
			Gln 86	Ar-H-Bond	2.48
			HOH 387	Ar-H-Bond	2.27
Formononetin	−6.47	−31.39	Gln 86	Ar-H-Bond	2.84
			HOH 322	Ar-H-Bond	2.61
Protein ID: 6FFC Inhibition capacity of human multidrug transporter ABCG2					
Robinin	−7.14	−53.99	Phe 439	H-Bond	1.85
			Asn 436	Ar-H-Bond	2.22
			Thr 402	Ar-H-Bond	2.57
			Thr 435	H-Bond	2.11
			Gln 368	H-Bond	2.40
Morin	−6.64	−34.48	Thr 402	H-Bond	1.68
			Phe 489	Ar-H-Bond	3.44
			Asn 436	H-Bond	1.78
Phloretin	−6.39	−34.84	Asn 436	H-Bond	1.86
			Phe 489	Ar-H-Bond	3.64
			Thr 402	Ar-H-Bond	2.56
Catechin	−6.36	−32.35	Thr 402	H-Bond	1.85
			Phe 489	Ar-H-Bond	3.23
			Phe 489	H-Bond	1.38
			Asn 436	Ar-H-Bond	2.22
			Asn 436	H-Bond	2.20
Phloretin	−6.36	−35.65	Thr 402	Ar-H-Bond	2.69
			Phe 489	Ar-H-Bond	3.63
			Asn 436	H-Bond	1.83
Protein ID: 3A4A Antifungal (*Saccharomyces cerevisiae*) by isomaltase inhibition					
Epigallocatechin	−6.98	−44.31	Glu 411	H-Bond	1.76
			Tyr 158	Ar-H-Bond	2.95
			Tyr 158	H-Bond	2.92
			Phe 314	Ar-H-Bond	3.12
			Phe 314	H-Bond H-Bond	3.51
			Asp 307	Ar-H-Bond	1.46
			Asp 307		2.60
Morin	−6.50	−40.65	Asp 307	H-Bond	1.69
			Gln 353	HBond Ar-H-Bond	1.79
			HOH 1207		2.46
Chrysin	−5.61	−34.69	Glu 411	Ar-H-Bond	2.79
			Tyr 158	H-Bond	1.92
			Gln 353	Ar-H-Bond	2.35
			Asp 307	Ar-H-Bond	2.25
Morin	−5.31	−38.38	Tyr 158	Ar-H-Bond	2.78
			Tyr 158	H-Bond	1.73
			Asp 307	Ar-H-Bond	2.50
			Gln 353	Ar-H-Bond	2.56
			Gln 353	H-Bond	1.80

Table 3 (*continued*)

Title	Docking Score	Glide Energy (Kcal/mol)	Interactions	Type	Bond length (Å)
Phloretin	−4.64	−38.76	Glu 411	H-Bond	2.43
			Asn 415	H-Bond	2.19
			Gln 353	H-Bond	2.10
Protein ID: 1IYL Antifungal (*Candida albicans*) by N-myristoyltransferase inhibition					
Epigallocatechingallate	−8.59	−58.16	Glu 109	Ar-H-bond	3.09
			Phe 339	Ar-H-bond	3.18
			Phe 115	Pi-Pi	4.39
			Asn 392	H-bond	2.07
			Tyr 225	Pi-Pi	4.16
			Tyr 356	Ar- H-bond	3.69
			Leu 451	2 H-bond	2.07, 1.88
			Tyr 107	H-bond	2.60
Neohesperidin	−8.55	−54.56	Asn 392	H-bond	1.96
			Tyr 354	2 Ar- H-bond	3.44, 3.64
			Tyr 335	H-bond	2.25
			Leu 45	H-bond	1.85
Biochanin A	−8.24	−41.78	Asn 392	Ar-H-bond	2.32
			Hie 227	H-bond	2.19
			Tyr 354	2 Pi-Pi	4.10, 4.13
			Tyr 225	2 Pi-Pi	4.11,4.86
Formononetin	−8.13	−38.64	Tyr 354	2 Pi-Pi	4.10, 4.13
			Tyr 225	2 Pi-Pi	4.11,4.86
			Hie 227	H-bond	2.24
			Asn 392	Ar-H-bond	2.33
Quercetin	−7.91	−44.10	Tyr 354	2 Pi-Pi	4.10, 4.13
			Tyr 225	2 Pi-Pi	4.11,4.86
			Hie 227	2 H-bond	2.59, 2.17
			Hie 227	Ar-H-bond	3.19
			Glu 109	H-bond	2.33
			Leu 451	H-bond	1.87
			Leu 450	H-bond	1.87
Protein ID: 1LRY Antibacterial (*Pseudomonas aeruginosa*) by Peptide Deformylase inhibition					
Silymarin	−8.82	−63.36	Glu 134	Ar- H-bond	2.53
			Ile 144	H-bond	1.84
			Pro 42	H-bond	1.85
Epigallocatechin	−7.90	−53.17	Glu 134	2 H-bond	1.55, 1.67
			Leu 92	H-bond	2.15
			Ile 44	H-bond	2.36
			Gln 88	H-bond	1.78
Naringenin	−7.38	−42.98	Glu 134	H-bond	1.56
			Glu 134	Ar-H-bond	2.35
			Gly 44	H-bond	1.69
			Gly 44	Ar-H-bond	2.69
			Tyr 87	Ar-H-bond	2.58
Quercetin	−7.29	−48.76	Glu 134	H-bond	1.67
			Glu 134	Ar-H-bond	2.48
			Gln 88	H-bond	1.76
Neohesperidin	−7.28	−60.23	Glu 134	H-bond	1.56
Protein ID: 2AIE Antibacterial (*Streptococcus pneumoniae*) by polypeptide deformylase inhibition					
Epigallocatechin	−6.40	−46.08	Gly 68	H-bond	1.70
			Leu 131	H-bond	2.21
			Glu 174	2 H-bond	1.64, 2.03
Catechin	−6.21	−44.36	Gly 68	Ar- H-bond	2.42
			Leu 131	H-bond	2.54
			Glu 174	H-bond	1.77
			Glu 174	Ar-H-bond	2.35
Robinin	−6.12	−64.85	Glu 125	H-bond	1.68
			Arg 67	H-bond	2.07
			Glu 174	2 H-bond	1.50, 1.78
Hesperidin	−5.93	−52.09	Glu 125	H-bond	1.60
			Arg 67	Pi-cation	5.98
Epigallocatechingallate	−5.88	−56.62	Gly 68	H-bond	1.77
			Glu 174	2 H-bond	1.92, 1.65

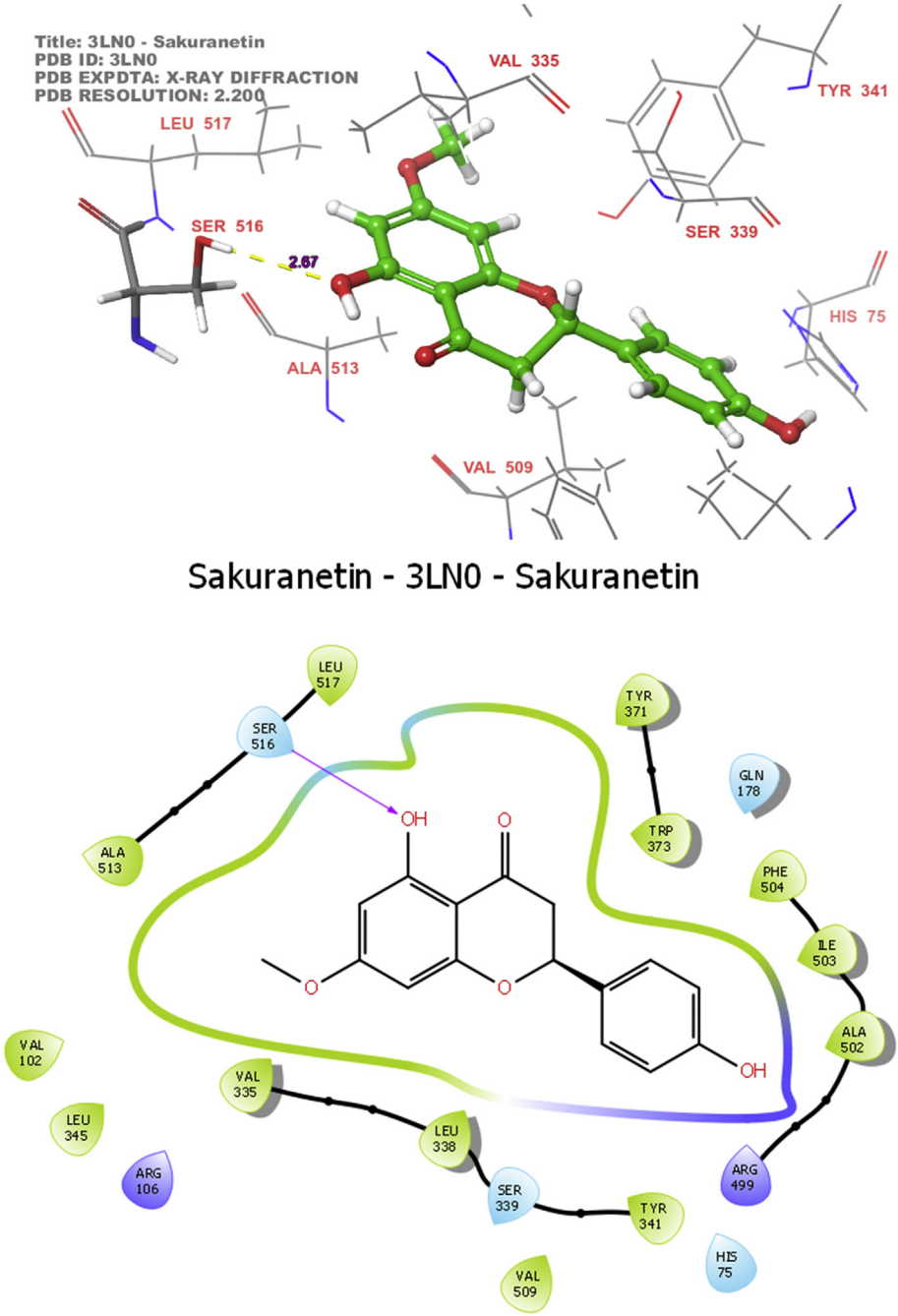

Fig. 1. 3D and 2D interactions of COX-2 (PDB ID: 3LN0) with flavonoid Sakuranetin. Figure shows Sakuranetin binding and interactions with human cyclo-oxygenase-2 with docking score of −7.31.

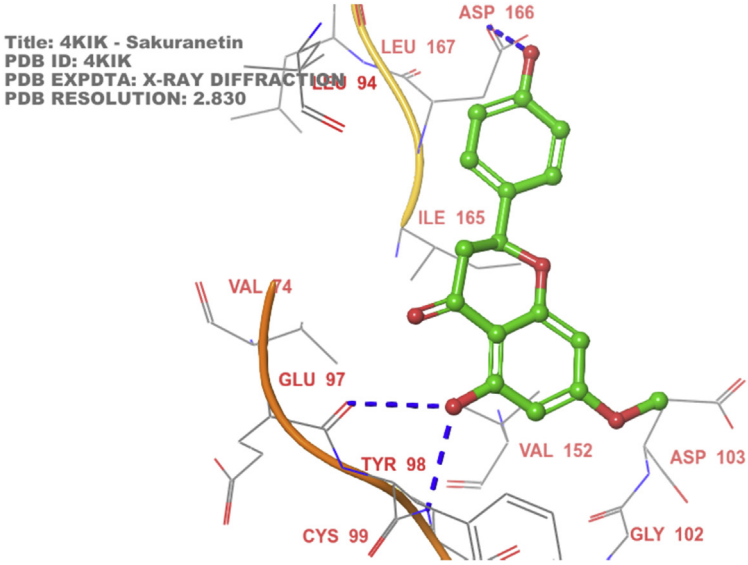

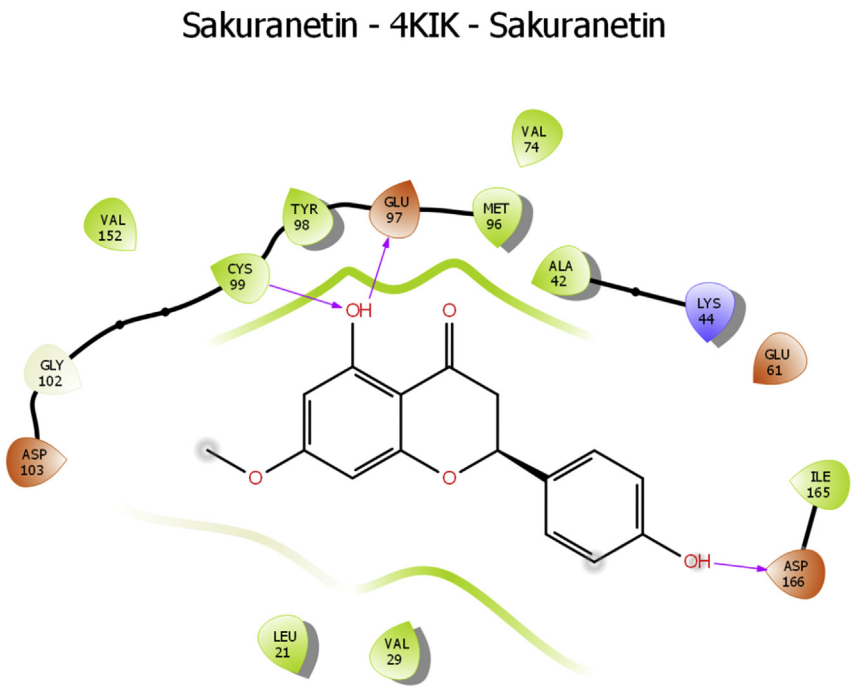

Fig. 2. 3D and 2D interactions of Human Ikb Kinase Beta (PDB ID: 4KIK) with flavonoid Sakuranetin. Figure shows Sakuranetin binding and interactions with Human Ikb Kinase Beta with docking score of −9.73.

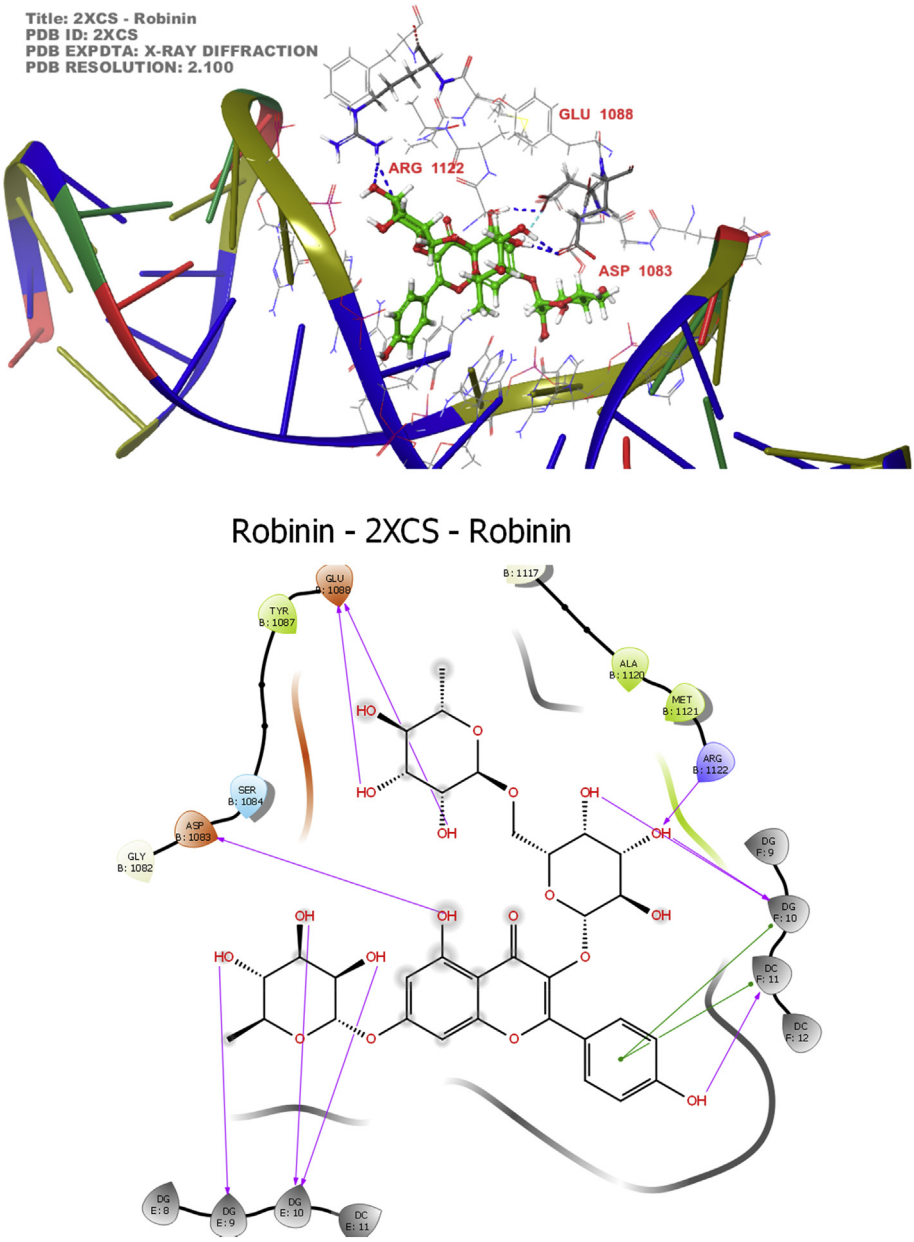

Fig. 3. 3D and 2D interactions of DNA gyrase (PDB ID: 2XCS) with Flavonoid Robinin. Figure shows Robinin binding and interactions with DNA gyrase *Staphylococcus aureus* with docking score of −8.03.

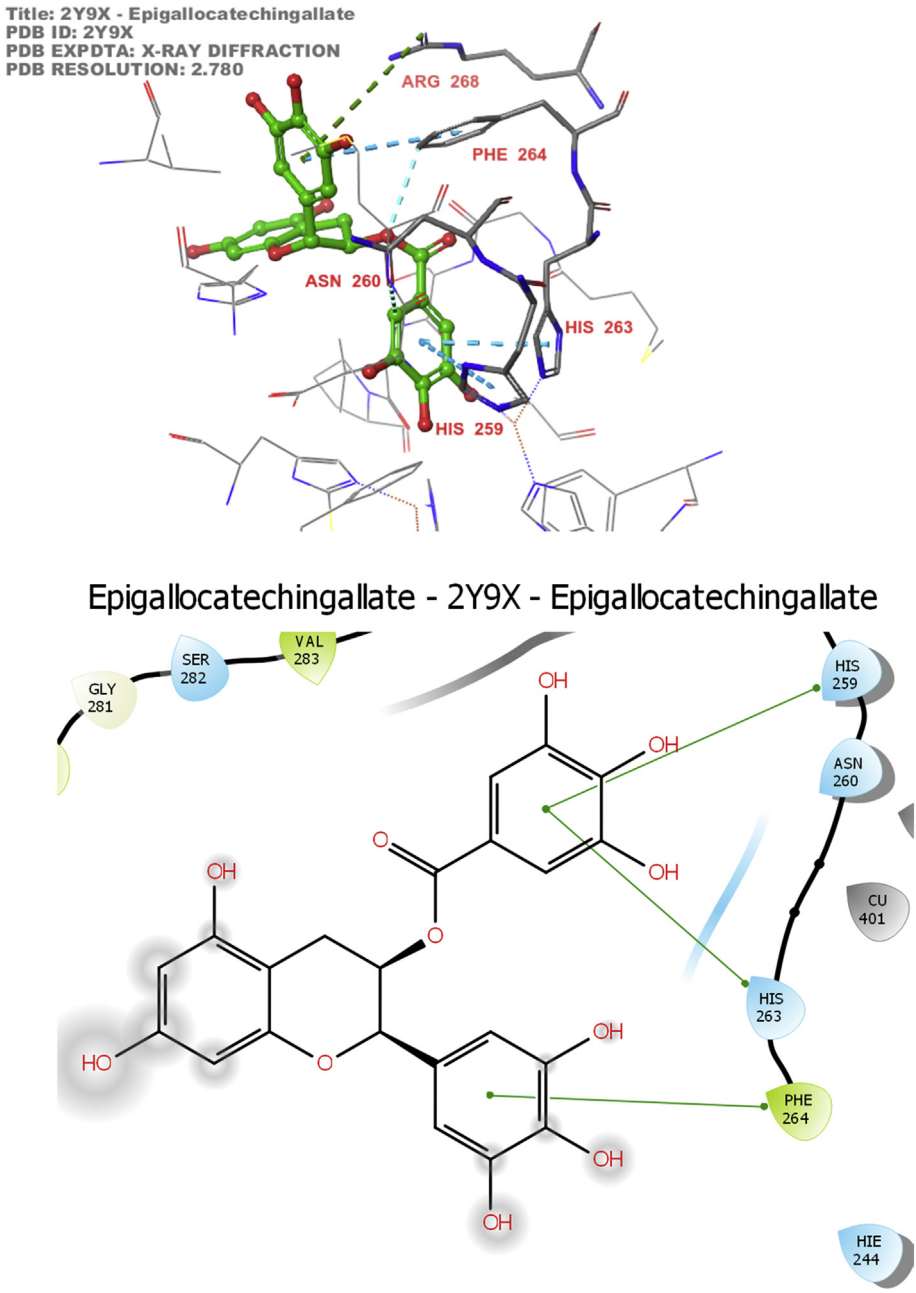

Fig. 4. 3D and 2D interactions of tyrosinase (PDB ID: 2Y9X) with flavonoid Epigallocatechingallate. Figure shows Epigallocatechingallate binding and interactions with *Agaricus bisporus* tyrosinase with docking score of −7.22.

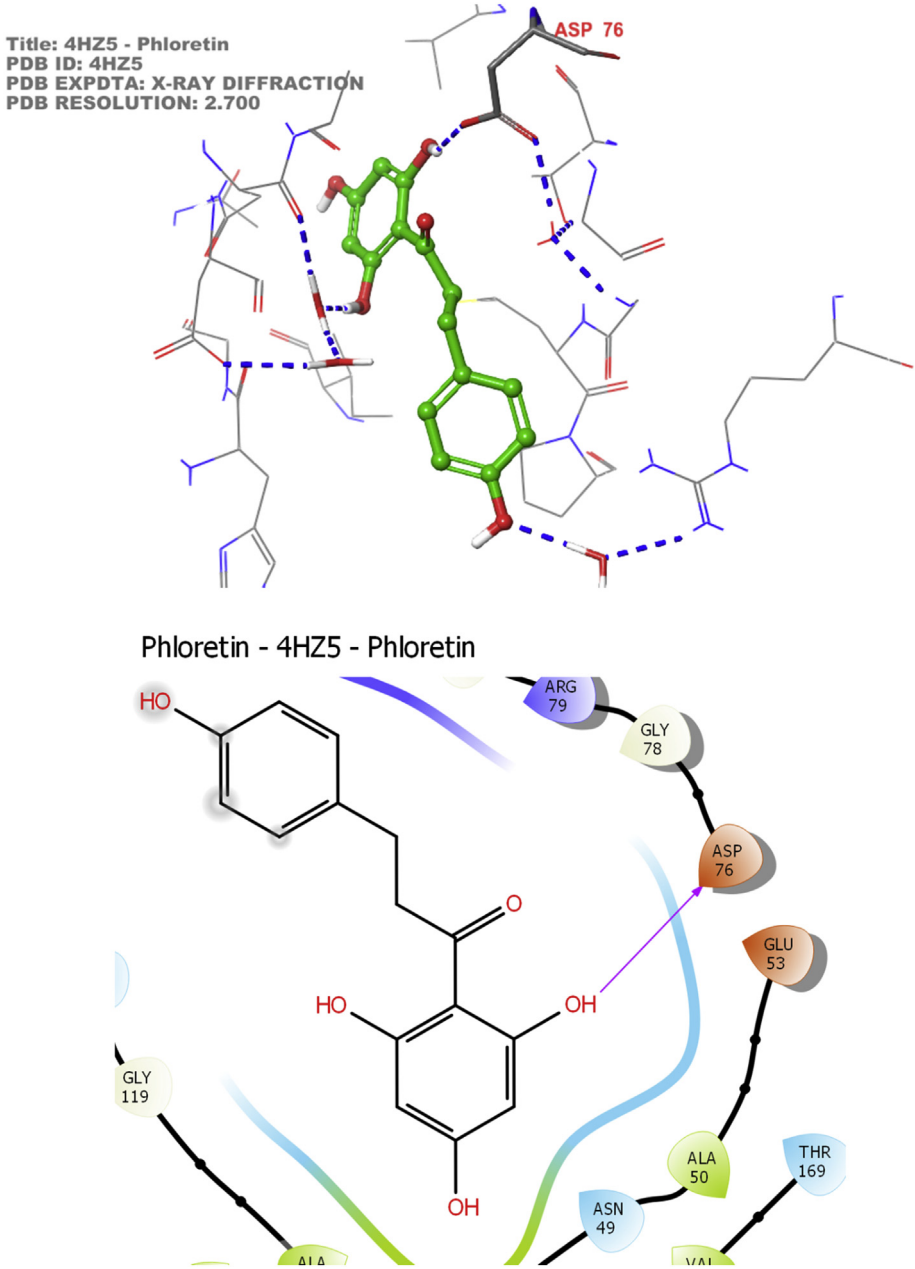

Fig. 5. 3D and 2D interactions of DNA gyrase (PDB ID: 4HZ5) with flavonoid Phloretin. Figure shows Phloretin binding and interactions with DNA gyrase with docking score of −7.06.

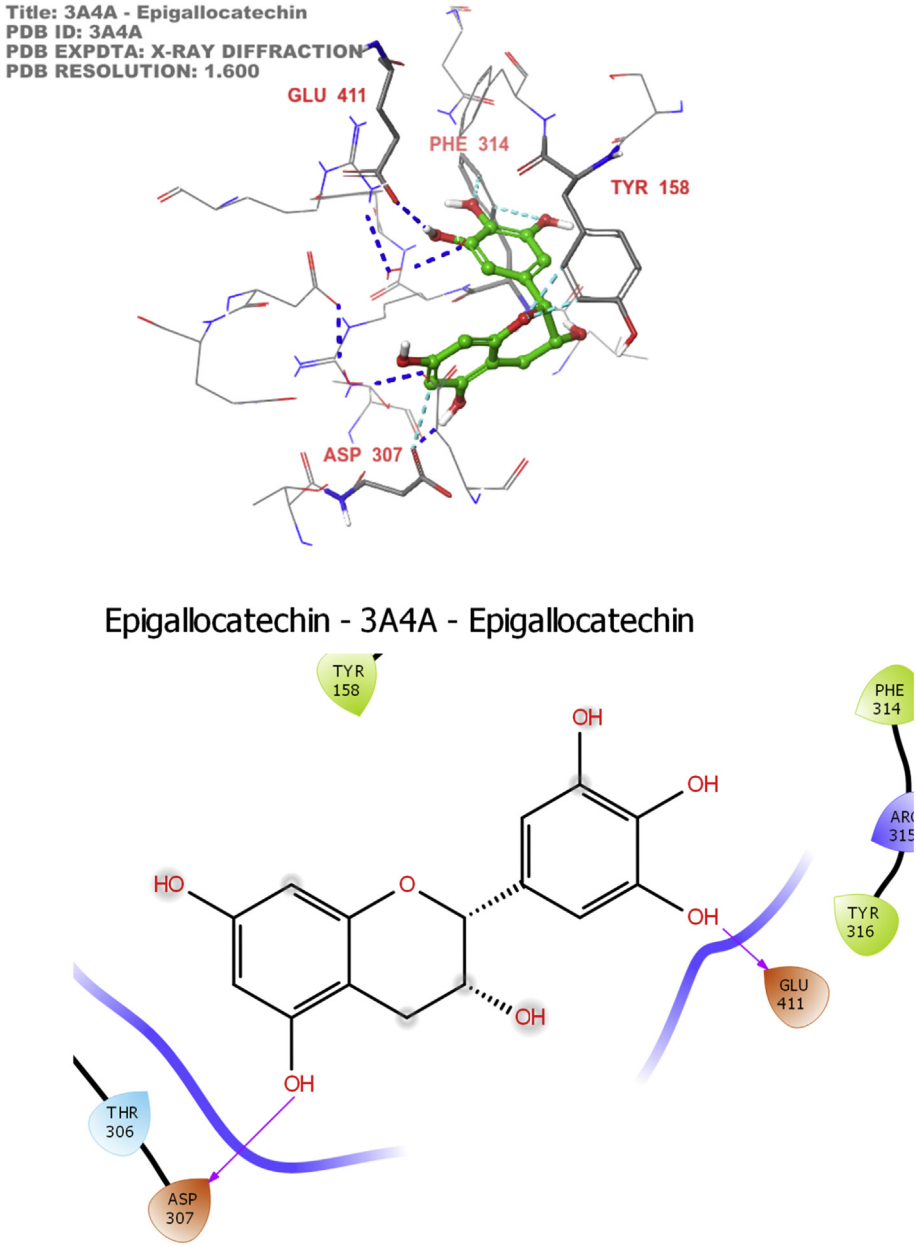

Fig. 6. 3D and 2D interactions of Isomaltase (PDB ID: 34A4) with flavonoid Epigallocatechin. Figure shows Epigallocatechin binding and interactions with Isomaltase of *Saccharomyces cerevisiae* with docking score of −6.98.

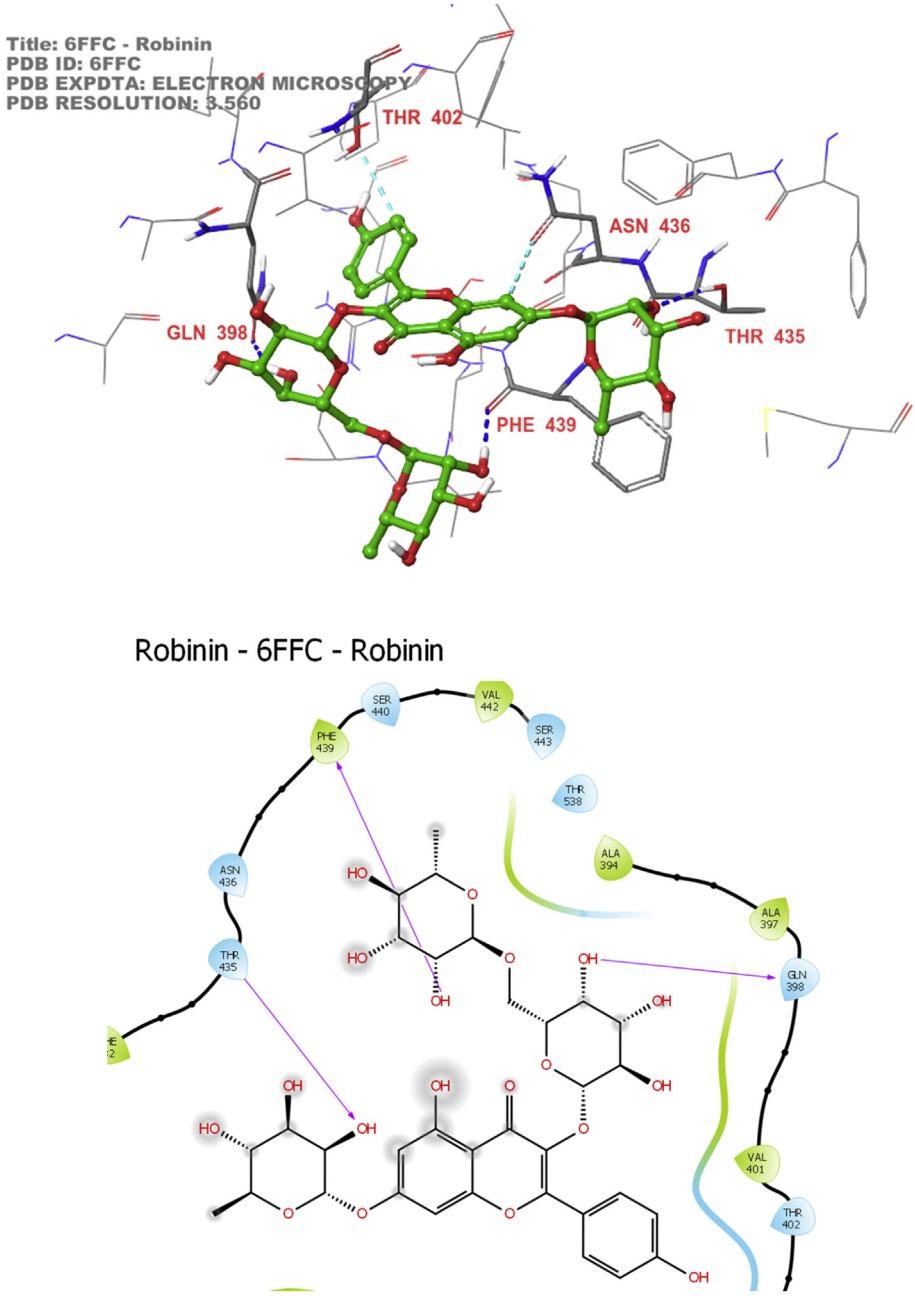

Fig. 7. 3D and 2D interactions of ABC transporter (PDB ID: 6FFC) with flavonoid Robinin. Figure shows Robinin binding and interactions with Human ABC transporter with docking score of −7.14.

minimized structures were docked on the prepared protein. The best flavonoid was identified based on the binding energy and interaction with amino acid residues for each protein.

Conflict of Interest

The authors declare that they have no known competing financial interests or personal relationships that could have appeared to influence the work reported in this paper.

Appendix A. Supplementary data

Supplementary data to this article can be found online at https://doi.org/10.1016/j.dib.2020.105243.

References

[1] J.L. Wang, D. Limburg, M.J. Graneto, J. Springer, J.R.B. Hamper, S. Liao, J.L. Pawlitz, R.G. Kurumbail, T. Maziasz, J.J. Talley, J.R. Kiefer, J. Carter, The novel benzopyran class of selective cyclooxygenase-2 inhibitors. Part 2: the second clinical candidate having a shorter and favorable human half-life, Bioorg. Med. Chem. Lett 20 (23) (2010) 7159–7163, https://doi.org/10.1016/j.bmcl.2010.07.054.

[2] N.S. Thomas, K. George, A.A.A. Selvam, Anticancer mechanism of troxerutin via targeting Nrf2 and NF-κB signalling pathways in hepatocarcinoma cell line, Toxicol. Vitro 54 (2019) 317–329, https://doi.org/10.1016/j.tiv.2018.10.018.

[3] L. Yao, L.-L. Wu, Q. Li, Q.-M. Hu, S.-Y. Zhang, K. Liu, J.-Q. Jiang, Novel berberine derivatives: design, synthesis, antimicrobial effects, and molecular docking studies, Chin. J. Nat. Med. 16 (10) (2018) 774–781, https://doi.org/10.1016/S1875-5364(18)30117-1.

[4] D. Szulczyk, M.A. Dobrowolski, P. Roszkowski, A. Bielenica, J. Stefańska, M. Koliński, S. Kmiecik, M. Jóźwiak, M. Wrzosek, W. Olejarz, M. Struga, Design and synthesis of novel 1H-tetrazol-5-amine based potent antimicrobial agents: DNA topoisomerase IV and gyrase affinity evaluation supported by molecular docking studies, Eur. J. Med. Chem. 156 (2018) 631–640, https://doi.org/10.1016/j.ejmech.2018.07.041.

[5] Y. Dong, X. Qiu, N. Shaw, Y. Xu, Y. Sun, X. Li, J. Li, Z. Rao, Molecular basis for the inhibition of β-hydroxyacyl-ACP dehydratase HadAB complex from *Mycobacterium tuberculosis* by flavonoid inhibitors, Protein & Cell 6 (7) (2015) 504–517, https://doi.org/10.1007/s13238-015-0181-1.

[6] C. Guerrero-Perilla, F.A. Bernal, E.D. Coy-Barrera, Molecular docking study of naturally occurring compounds as inhibitors of N-myristoyl transferase towards antifungal agents discovery, Rev. Colomb. Ciencias Quím. Farm. 44 (2) (2015) 162–178, https://doi.org/10.15446/rcciquifa.v44n2.56291.

[7] S. Fieulaine, R. Alves de Sousa, L. Maigre, K. Hamiche, M. Alimi, J.-M. Bolla, A. Taleb, A. Denis, J.-M. Pagès, I. Artaud, T. Meinnel, C. Giglione, A unique peptide deformylase platform to rationally design and challenge novel active compounds, Sci. Rep. 6 (1) (2016) 35429, https://doi.org/10.1038/srep35429.

[8] H. Liu, Y. Zhu, T. Wang, J. Qi, X. Liu, Enzyme-site blocking combined with optimization of molecular docking for efficient discovery of potential tyrosinase specific inhibitors from *Puerariae lobatae* radix, Molecules 23 (10) (2018) 2612, https://doi.org/10.3390/molecules23102612.

[9] S. Murugesu, Z. Ibrahim, Q.-U. Ahmed, N.-I. Nik Yusoff, B.-F. Uzir, V. Perumal, F. Abas, K. Saari, H. El-Seedi, A. Khatib, Characterization of α-glucosidase inhibitors from *Clinacanthus nutans* Lindau leaves by gas chromatography-mass spectrometry-based metabolomics and molecular docking simulation, Molecules 23 (9) (2018) 2402, https://doi.org/10.3390/molecules23092402.

[10] S.M. Jackson, I. Manolaridis, J. Kowal, M. Zechner, N.M.I. Taylor, M. Bause, S. Bauer, R. Bartholomaeus, G. Bernhardt, B. Koenig, A. Buschauer, H. Stahlberg, K.-H. Altmann, K.P. Locher, Structural basis of small-molecule inhibition of human multidrug transporter ABCG2, Nat. Struct. Mol. Biol. 25 (4) (2018) 333–340, https://doi.org/10.1038/s41594-018-0049-1.